PNAS RESEARCH ARTICLE | IMMUNOLOGY AND INFLAMMATION

Endocytosis triggers V-ATPase-SYK–mediated priming of cGAS activation and innate immune response

Yu-Lin Yang[a,1], Li-Bo Cao[a,1], Wen-Rui He[a,1], Li Zhong[a], Yi Guo[a], Qing Yang[a], Hong-Bing Shu[a,b], and Ming-Ming Hu[a,b,2]

Edited by Katherine Fitzgerald, University of Massachusetts Medical School, Worcester, MA; received April 27, 2022; accepted September 2, 2022

The current view of nucleic acid–mediated innate immunity is that binding of intracellular sensors to nucleic acids is sufficient for their activation. Here, we report that endocytosis of virus or foreign DNA initiates a priming signal for the DNA sensor cyclic GMP-AMP synthase (cGAS)–mediated innate immune response. Mechanistically, viral infection or foreign DNA transfection triggers recruitment of the spleen tyrosine kinase (SYK) and cGAS to the endosomal vacuolar H^+ pump (V-ATPase), where SYK is activated and then phosphorylates human cGAS$^{Y214/215}$ (mouse cGas$^{Y200/201}$) to prime its activation. Upon binding to DNA, the primed cGAS initiates robust cGAMP production and mediator of IRF3 activation/stimulator of interferon genes-dependent innate immune response. Consistently, blocking the V-ATPase-SYK axis impairs DNA virus- and transfected DNA-induced cGAMP production and expression of antiviral genes. Our findings reveal that V-ATPase-SYK–mediated tyrosine phosphorylation of cGAS following endocytosis of virus or other cargos serves as a priming signal for cGAS activation and innate immune response.

antiviral innate immunity | DNA sensor cGAS | signal transduction | phosphorylation modification

Significance

The current view of nucleic acid–mediated innate immunity is that binding of nucleic acids is sufficient for the activation of intracellular sensors. In this study, our findings suggest a "dual-signal" model for effective cGAS activation, which includes the first V-ATPase-SYK–mediated priming signal during endocytosis and the second DNA stimulatory signal. Mechanistically, viral infection or foreign DNA transfection triggers recruitment of the spleen tyrosine kinase (SYK) and cGAS to the endosomal vacuolar H^+ pump (V-ATPase), where SYK is activated and then phosphorylates human cGAS$^{Y214/215}$ (mouse cGas$^{Y200/201}$) to prime its activation. Upon binding to DNA, the primed cGAS initiates robust cGAMP production and MITA/STING-dependent innate immune response. This renews our understanding of intracellular nucleic acid sensor-mediated innate immunity.

How viruses invade host cells has been elucidated in past decades. Except for a small fraction of enveloped viruses that invade cells through direct fusion of viral envelopes with the plasma membrane, the majority of viruses invade the host cells via endocytosis (1, 2). After reaching to endocytic vesicles or early endosomes, at where the vacuolar H^+-ATPase (V-ATPase) assembles and acts as an ATP-driven electrogenic proton pump to alter the pH of their cavities, these viruses escape from endocytic vesicles or endosomes into the cytosol, commonly in a low pH-dependent manner (3). Similar processes are also essential for delivery of foreign substances, including nucleic acids by carrier materials, such as lipofectamine (LF) and polyetherimide (PEI) (4). Whereas the function and mechanism of viral endocytosis and endosomal escape have been well documented, it is unknown whether these processes are sensed by the immune surveillance machinery of the host.

How the host cell defends viral infection is a key question of biology. In the past years, it has been well established that the cytoplasmic cyclic GMP-AMP synthase (cGAS) is a critical innate immune sensor for viral DNA, mitochondrial DNA (mtDNA), and cellular nuclear DNA (nuDNA) dislocated in the cytosol upon infection of certain viruses or other cellular stresses (5, 6). Upon binding to DNA, the cGAS-DNA complex undergoes phase separation to form cGAS-DNA liquid droplets, in which cGAS utilizes GTP and ATP as substrates to synthesize cyclic GMP-AMP (cGAMP) (7, 8). cGAMP then acts as a second messenger (9), which binds to and activates the endoplasmic reticulum (ER)-associated protein MITA (mediator of IRF3 activation), also called STING (stimulator of interferon genes) (10, 11). MITA/STING recruits the kinase TBK1 and the transcription factor IRF3, leading to induction of type I interferons (IFNs) and other effector genes (5). The downstream cytokines and effectors inhibit viral replication or induce apoptosis of infected cells, leading to innate antiviral response (12, 13).

Although cGAS senses both foreign DNA and self-DNA, there is a large difference between the immune outcomes from these two kinds of ligands. For example, DNA virus infection or DNA transfection usually triggers robust production of cGAMP and induction of type I IFNs in host cells (8), while self-DNA exposure (including cytosolic mtDNA and nuDNA) only elicits a mild IFN response under physiological conditions (14), which suggests differential activation of cGAS-MITA/STING–mediated innate immune response triggered by foreign and self-DNA. In this context, cGAS is reported to be predominantly located at the plasma membrane via binding to $PI(3,5)P_2$ to avoid sensing of cytosolic self-DNA, especially in phagocytes (15), which represents a "passive" protective strategy through cGAS-DNA physical isolation. Mutation of $PI(3,5)P_2$ binding sites of cGAS expectedly increases the intrinsic type I IFN levels, but

Author contributions: Y.-L.Y., H.-B.S., and M.-M.H. designed research; Y.-L.Y., L.-B.C., W.-R.H., L.Z., and Y.G. performed research; Y.-L.Y., L.-B.C., W.-R.H., Q.Y., H.-B.S., and M.-M.H. analyzed data; and Y.-L.Y., H.-B.S., and M.-M.H. wrote the paper.

The authors declare no competing interest.

This article is a PNAS Direct Submission.

[1]Y.-L.Y., L.-B.C., and W.-R.H. contributed equally to this work.

[2]To whom correspondence may be addressed. Email: mmhu@whu.edu.cn.

This article contains supporting information online at http://www.pnas.org/lookup/suppl/doi:10.1073/pnas.2207280119/-/DCSupplemental.

Published October 17, 2022.

impairs viral infection-triggered expression of antiviral genes (15). This implies that there are some cell membrane-associated molecular events that govern cGAS-mediated innate immune response to foreign viral DNA, which remains largely unknown. Additionally, virus–cell membrane fusion is reported to trigger innate immune response via induction of mtDNA release into cytosol, which induces cGAS-MITA/STING–dependent innate immunity (16, 17). Whether virus–cell interaction affects activities of cGAS-MITA/STING signaling is not reported in previous studies.

In this study, we report that endocytosis of virus or foreign DNA initiates a priming signal for activation of the DNA sensor cGAS. Viral endocytosis triggers recruitment of the tyrosine kinase SYK (spleen tyrosine kinase) and cGAS to the endosomal V-ATPase, where SYK is activated and then phosphorylates cGAS $^{Y214/215}$ (mouse cGas$^{Y200/201}$) to prime its activation. Upon binding to DNA, the primed cGAS initiates robust cGAMP production and MITA/STING-dependent innate immune response. Our findings suggest a "dual-signal" model for effective cGAS activation, which includes the first priming signal and the second DNA stimulatory signal.

Results

SYK Promotes Innate Immune Response Triggered by Endocytosed Foreign DNA. It has been well established that certain tyrosine kinases play roles in cell membrane-associated signal transduction upon extracellular stimulation. To elucidate cell membrane-associated molecular events that govern cGAS-MITA/STING–mediated innate immunity, we screened a pool of tyrosine kinase inhibitors to examine their effects on transcription of *Ifnb1* induced by infection with the DNA virus herpes simplex virus 1 (HSV-1) or transfection of HT-DNA, which are endocytosed from the extracellular environment into the cytoplasm. We have also examined the effects of these tyrosine kinase inhibitors on transcription of *Ifnb1* induced by a combination (A/Q) of chemical compounds, including the apoptosis inducer ABT-737 (A) and the pan-caspase inhibitor Q-VD-OPH (Q), which can diffuse from the extracellular environment into the cytoplasm and induce mtDNA release to trigger cGAS-MITA/STING–dependent innate immunity (14, 18, 19). In these experiments, both cGAS inhibitor (RU.521) and MITA/STING inhibitor (STING-IN-3) suppressed transcription of the *Ifnb1* gene induced by HSV-1 infection, HT-DNA transfection, and A/Q treatment (Fig. 1*A*). Two selective inhibitors of Syk, PRT062607 and BAY61-3606 (20, 21), markedly inhibited transcription of the *Ifnb1* gene induced by HSV-1 infection and HT-DNA transfection but had no marked effects on A/Q-induced transcription of the *Ifnb1* gene (Fig. 1*A*). In similar experiments, Syk inhibitors did not suppress IFN-γ–induced transcription of the *Irf1* gene in Raw264.7 cells (*SI Appendix*, Fig. S1*A*). Syk inhibitor PRT062607 also suppressed transcription of *Ifnb1* and other downstream antiviral genes, including *Ifit1* and *Cxcl10* induced by HSV-1 infection and HT-DNA transfection, but not A/Q treatment in primary mouse bone marrow-derived dendric cells (BMDCs) (Fig. 1*B*) and human THP-1 cells (*SI Appendix*, Fig. S1*B*). Additionally, the Syk inhibitor had no marked effects on IFN-γ–induced transcription of the *IRF1* gene in BMDCs and THP-1 cells (Fig. 1*C* and *SI Appendix*, Fig. S1*C*). These results suggest that tyrosine kinase SYK is involved in innate immunity triggered by endocytosed foreign DNA but not endogenous mtDNA.

To confirm our hypothesis, we generated Syk-deficient cells by the CRISPR-Cas9 system (Fig. 1*D* and *SI Appendix*, Fig. S1*D*). Consistently, Syk-deficiency inhibited transcription of the *Ifnb1* gene induced by HSV-1 infection, HT-DNA transfection, but not A/Q treatment in both Raw264.7 and THP-1 cells (Fig. 1*E* and *SI Appendix*, Fig. S1*D*). SYK-deficiency also had no marked effects on IFN-γ–induced transcription of the *IRF1* gene in these cells (Fig. 1*F* and *SI Appendix*, Fig. S1*E*). Biochemically, Syk-deficiency markedly inhibited phosphorylation of Tbk1^{S172} and Irf3^{S388} induced by HSV-1 infection and HT-DNA transfection (Fig. 1*G*), which are hallmarks for activation of nucleic acid-triggered innate immune signaling (5). Consistent with the impaired innate immune response in Syk-deficient cells, much higher levels of HSV-1 *UL1* and *UL49* genes were detected in Syk-deficient compared to control cells (*SI Appendix*, Fig. S1*F*). Collectively, these results suggest that Syk positively regulates endocytosed foreign DNA- but not endogenous mtDNA-triggered innate immunity.

We further evaluated the physiological functions of Syk in antiviral innate immune response to DNA virus in mice. The in vivo experiments showed that intraperitoneal injection of PRT062607 dramatically inhibited secretion of Ifn-β and Cxcl10 in the serum of HSV-1–infected mice (Fig. 1*H*), as well as transcription of the *Ifnb1* gene in the liver and lung of infected mice (*SI Appendix*, Fig. S1*G*). Consistently, administration of PRT062607 led to higher HSV-1 titers in the mouse brains and earlier onset and marked higher rates of death of mice after HSV-1 infection intravenously (Fig. 1 *I* and *J*). Since HSV-1 is a neurotropic virus and a major cause of central nervous system (CNS) infections, including herpes simplex encephalitis (22), and the cGAS-MITA/STING–mediated type I IFN production in microglia is critical for viral defense in the CNS (23). Therefore, we further evaluated the role of SYK in antiviral innate immune response in the CNS. The results showed that PRT062607 treatment also inhibited expression of antiviral genes in microglia BV2 cells. Furthermore, by utilizing an ocular infection model, we also detected an increase of HSV-1 titers in the brainstems of mice after HSV-1 infection (*SI Appendix*, Fig. S1 *H* and *I*). Collectively, these results suggest that Syk is critical for host defense against DNA virus in vivo.

Syk Mediates Tyrosine Phosphorylation of cGas. We next investigated the mechanism on how Syk regulates innate immunity triggered by endocytosed foreign DNA. cGAS activity assays indicated that the Syk inhibitor PRT062607 dramatically reduced cGAMP production induced by HT-DNA transfection (Fig. 2*A*). However, PRT062607 could not inhibit cGAMP-induced transcription of *Ifnb1* and *Ifit1* genes (Fig. 2*B*). Consistently, Syk-deficiency also markedly inhibited cGAMP production induced by HT-DNA transfection (Fig. 2*C*), while hardly affecting cGAMP-induced transcription of antiviral genes, as well as activation of MITA/STING signaling indicated by phosphorylation of Mita^{S365}, Tbk1^{S172}, and Irf3^{S388} in Raw264.7 cells (Fig. 2 *D* and *E*). Mammalian overexpression and coimmunoprecipitation experiments showed that human SYK interacted with cGAS (Fig. 2*F*). Endogenous SYK and cGAS were barely associated with each other but their association was induced following HSV-1 infection in both Raw264.7 and THP-1 cells (Fig. 2 *G* and *H*). In these experiments, activation of antiviral innate immune signaling following HSV-1 infection was indicated by phosphorylation of TBK1^{S172} in these cells (Fig. 2 *G* and *H*). These data suggest that Syk regulates endocytosed foreign DNA-triggered innate immunity by targeting cGas.

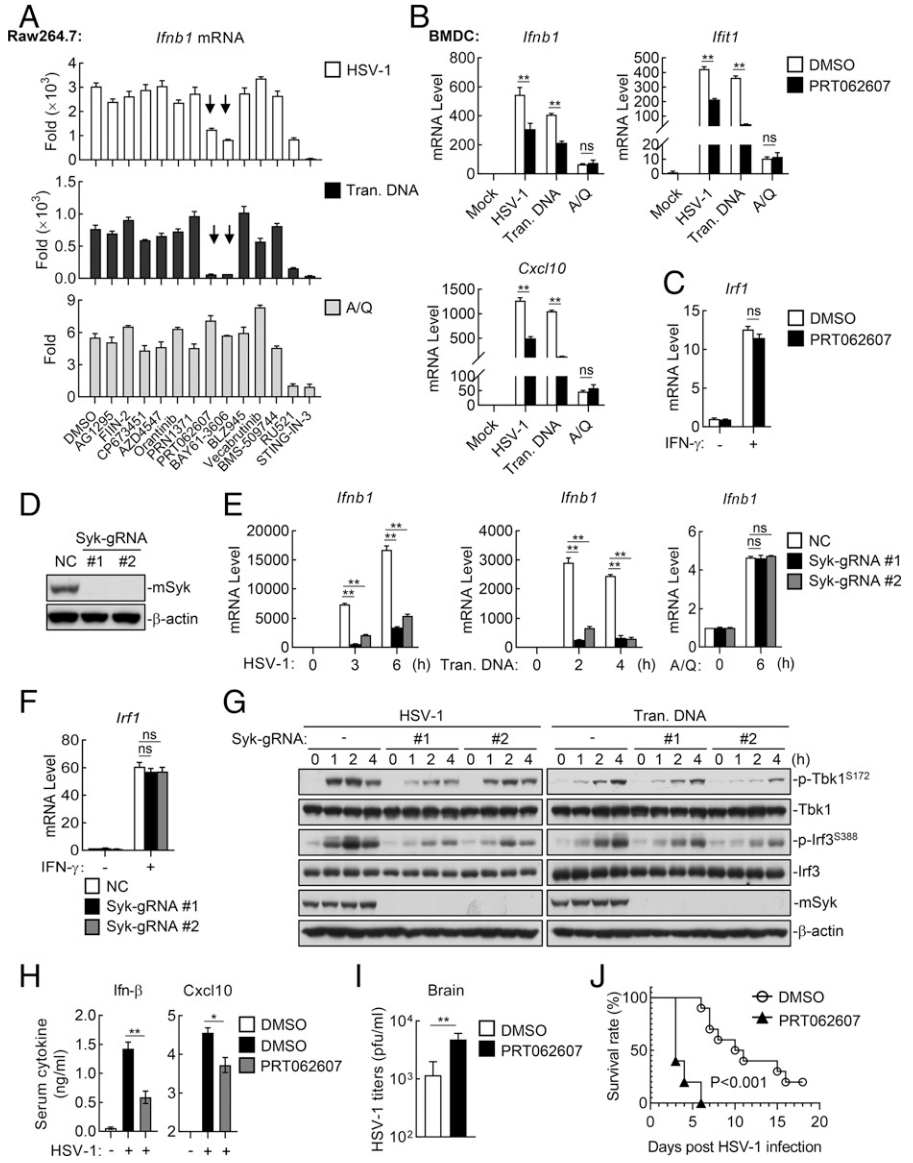

Fig. 1. Syk promotes innate immune response triggered by endocytosed foreign DNA. (*A*) Screening of tyrosine kinases that regulate transcription of *Ifnb1* induced by endocytosed foreign DNA. Raw264.7 cells (1×10^6) were pretreated with each chemical inhibitor for half an hour, and then treated with HSV-1 (multiplicity of infection [MOI] = 1) for 6 h, transfected with HT-DNA (1 μg/mL) for 4 h, or treated with A/Q (10 μM each) for 6 h, followed by qPCR analysis of *Ifnb1* mRNA level. Tran. DNA, transfected HT-DNA. (*B*) Effects of SYK inhibitor on transcription of downstream antiviral genes induced by endocytosed foreign DNA. BMDCs (1×10^6) were pretreated with DMSO or PRT062607 (10 μM) for half an hour, and then left untreated or treated with HSV-1 (MOI = 1) for 6 h, transfected with HT-DNA (1 μg/mL) for 4 h, or treated with A/Q (10 μM each) for 6 h, followed by qPCR analysis of the indicated genes. (*C*) Effect of SYK inhibitor on IFN-γ–induced transcription of the *Irf1* gene in BMDCs. BMDCs (1×10^6) were pretreated with DMSO or PRT062607 (10 μM) for half an hour, and then left untreated or treated with IFN-γ (100 ng/mL) for 4 h, followed by qPCR analysis of the *Irf1* gene. (*D* and *E*) Effects of Syk-deficiency on endocytosed DNA-induced transcription of the *Ifnb1* gene. (*Left*) The negative control (NC) and Syk-gRNA stably transduced Raw264.7 cells were lysed for immunoblot analysis with the indicated antibodies to examine the KO efficiency. (*Right*) The NC and Syk-gRNA stably transduced Raw264.7 cells (1×10^6) were left untreated or treated with HSV-1 (MOI = 1) for 6 h, transfected with HT-DNA (1 μg/mL) for 4 h, or treated with A/Q (10 μM each) for 6 h, followed by qPCR analysis of the *Ifnb1* gene. (*F*) Effect of Syk-deficiency on IFN-γ–induced transcription of the *Irf1* gene. The NC and Syk-deficient RAW264.7 cells (1×10^6) were left untreated or treated with IFN-γ (100 ng/mL) for 4 h, followed by qPCR analysis of the *Irf1* gene. (*G*) Effects of Syk-deficiency on endocytosed DNA-induced phosphorylation of Tbk1 and Irf3. The NC and Syk-deficient RAW264.7 cells (1×10^6) were treated with HSV-1 (MOI = 2), or transfected with HT-DNA (1 μg/mL) for the indicated times before immunoblot analysis with the indicated antibodies. (*H*) Effects of SYK inhibitor on HSV-1–induced production of Ifn-β and Cxcl10 in serum. Mice ($n = 3$) were intraperitoneally injected with DMSO or PRT062607 (30 mg/kg) for half an hour, and then left untreated or injected intravenously with HSV-1 (KOS strain, 5×10^7 pfu) for 6 h, followed by orbital blood collection for ELISA. (*I*) Measurement of viral titers in the brains of mice. Mice ($n = 5$) were intraperitoneally mock-injected or injected with PRT062607 (30 mg/kg) for half an hour, and then injected intravenously with HSV-1 (KOS strain, 5×10^7 pfu) for 4 d. HSV-1 viral titers in the brains of infected mice were quantified by plaque assays. (*J*) Effect of SYK inhibitor on HSV-1 infection-induced death of mice. Mice ($n = 10$) were intraperitoneally mock-injected or injected with PRT062607 (30 mg/kg) for half an hour, and then injected intravenously with HSV-1 (KOS strain, 5×10^7 pfu), followed by mice survival record for 2 wk. *P* value of the survival rate is analyzed by log-rank (Mantel–Cox) test. ns, nonsignificant; $^*P < 0.05$, $^{**}P < 0.01$ (unpaired *t* test). The data shown are the mean ± SD ($n = 3$). All experiments were performed at least two times.

We next determined whether HSV-1 infection, which is mainly via endocytosis, activates Syk. Immunoblots indicated that HSV-1 infection induced dynamic phosphorylation of mouse Syk at Y519/520 (corresponding to Y525/526 of human SYK), a hallmark of Syk activation, which is peaked at 60 min postinfection in Raw264.7 cells (Fig. 2*I*). Overexpression of human SYK, but not its enzyme-inactive mutant SYK(D494A), dramatically increased tyrosine phosphorylation of human cGAS in biochemical experiments (Fig. 2*J*). Three conserved residues of human cGAS—including Y214, Y215, and Y483—were preferentially targeted by human SYK as analyzed by mass spectrometry (MS) (Fig. 2*K* and *SI Appendix*, Fig. S2*A*). Consistently, mutation of

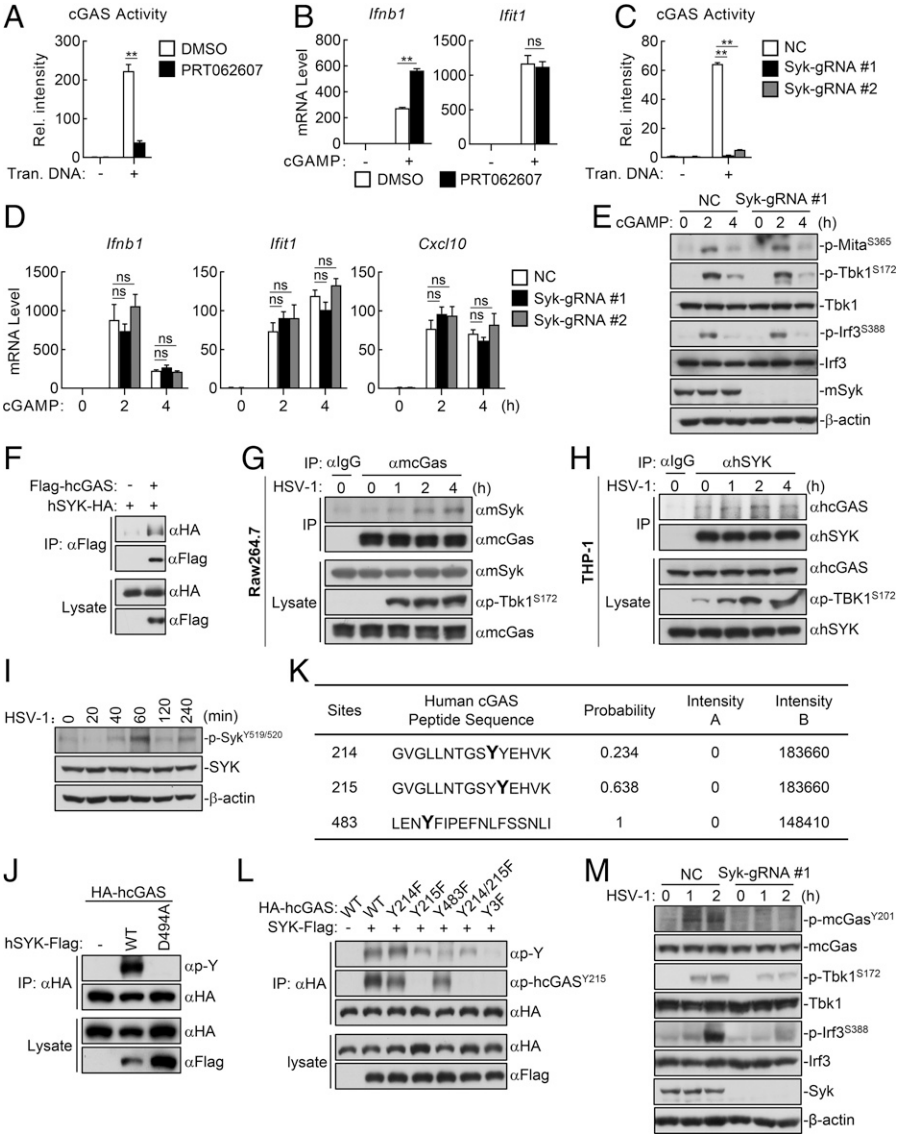

Fig. 2. Syk mediates tyrosine phosphorylation of cGas. (*A*) Effect of SYK inhibitor on cGAS activity. Raw264.7 cells (2×10^7) were pretreated with DMSO or PRT062607 (10 μM) for half an hour, and then left mock-transfected or transfected with HT-DNA (1 μg/mL) for 4 h, followed by cGAMP activity assay. (*B*) Effect of SYK inhibitor on transcription of downstream antiviral genes induced by cGAMP. Raw264.7 cells (1×10^6) were pretreated with DMSO or PRT062607 (10 μM) for half an hour, and then left untreated or treated with 2′3′-cGAMP (0.2 μg/mL) for 4 h, followed by qPCR analysis of the indicated genes. (*C*) Effect of Syk-deficiency on cGAS activity. The NC and Syk-deficient RAW264.7 cells (2×10^7) were left mock-transfected or transfected with HT-DNA (1 μg/mL) for 4 h, followed by cGAMP activity assay. (*D*) Effect of Syk-deficiency on transcription of downstream antiviral genes induced by cGAMP. The NC and Syk-deficient RAW264.7 cells (1×10^6) were left untreated or treated with 2′3′-cGAMP (0.2 μg/mL) for 4 h, followed by qPCR analysis of the indicated genes. (*E*) Effects of Syk-deficiency on cGAMP-induced phosphorylation of Mita, Tbk1, and Irf3. The NC and Syk-deficient RAW264.7 cells (1×10^6) were left untreated or treated with 2′3′-cGAMP (0.2 μg/mL) for the indicated times before immunoblot analysis with the indicated antibodies. (*F*) Association of human SYK with cGAS in overexpression system. HEK293 cells (1×10^7) were transfected with the indicated plasmids for 20 h, and then cells were lysed for coimmunoprecipitation with Flag antibody, followed by immunoblot analysis with the indicated antibodies. (*G* and *H*) Association of endogenous SYK with cGAS following viral infection. RAW264.7 and THP-1 cells (5×10^7) were left uninfected or infected with HSV-1 (MOI = 2) for the indicated times before cells were harvested for immunoprecipitation with control IgG, cGas or SYK antibody. The lysates and immunoprecipitates were subjected to immunoblot analysis with the indicated antibodies. (*I*) Activation of mouse Syk by viral infection. Raw264.7 cells (1×10^6) were left untreated or treated with HSV-1 (MOI = 2) for the indicated times before immunoblot analysis with the indicated antibodies. (*J*) Effects of human SYK and its mutant SYK (D494A) on the tyrosine phosphorylation of cGAS. HEK293 cells (1×10^7) were transfected with the indicated plasmids for 20 h, and then cells were lysed for coimmunoprecipitation with HA antibody, followed by immunoblot analysis with the indicated antibodies. (*K*) Identification of SYK-phosphorylated peptides of human cGAS by MS. HEK293 cells (1×10^8) were transfected with HA-tagged human cGAS (sample A) or transfected with HA-tagged human cGAS and SYK together (sample B) for 20 h, and then cells were lysed for immunoprecipitation with HA antibody. The precipitates were subjected to MS. The phosphorylated peptides of cGAS detected in sample B but not A is shown in the table. (*L*) Effects of SYK on the tyrosine phosphorylation of human cGAS and its mutants. HEK293 cells (1×10^7) were transfected with the indicated plasmids for 20 h, and then cells were lysed for coimmunoprecipitation with HA antibody, followed by immunoblot analysis with the indicated antibodies. (*M*) Effects of Syk-deficiency on viral infection-induced phosphorylation of mouse cGas^{Y201}. The NC or SYK-deficient RAW264.7 cells (1×10^6) were left untreated or treated with HSV-1 (MOI = 2) for the indicated times, followed by immunoblot analysis with the indicated antibodies. ns, nonsignificant; $^{**}P < 0.01$ (unpaired *t* test). The data shown are the mean ± SD ($n = 3$). All experiments were performed at least two times.

each of these residues to phenylalanine (F) individually decreased phosphorylation of cGAS by SYK, while simultaneous mutation of all three residues abolished tyrosine phosphorylation of cGAS by SYK (Fig. 2*L*). Immunoblots with an antibody specific for Y215-phosphorylated human cGAS (p-cGAS^{Y215}) (24) indicated that SYK increased phosphorylation of human cGAS at Y215 but had no effects on cGAS^{Y215F} (Fig. 2*L*). Importantly, immunoblots indicated that HSV-1 infection caused phosphorylation of endogenous mouse cGas at Y201 (corresponding to Y215 of human cGAS) at 1 to 2 h in control cells, which was markedly

down-regulated in Syk-deficient Raw264.7 cells and abolished in cGas-deficient cells (Fig. 2*M* and *SI Appendix*, Fig. S2*B*). In these experiments, HSV-1–induced phosphorylation of $Tbk1^{S172}$ at 1 to 2 h and $Irf3^{S388}$ at 2 h were also impaired in Syk-deficient cells (Fig. 2*M*), which is consistent with our previous results (Fig. 1*G*). Taken together, these results suggest that Syk is activated following HSV-1 infection and mediates tyrosine phosphorylation of cGas.

Phosphorylation of Human cGAS at Y214/215 Is Critical for cGAS Activation. We next investigated the functions of tyrosine phosphorylation of cGAS at these resides. Luciferase reporter assays indicated that individual mutation of Y214 or Y215 of human cGAS to phenylalanine inhibited its ability to activate the IFN-β promoter and simultaneous mutation of Y214 and Y215 of human cGAS to phenylalanines (Y214/215F) further impaired its activity (Fig. 3*A*). However, mutation of Y483 to phenylalanine had no marked effects on cGAS activity (Fig. 3*A*). These results indicated that phosphorylation of human cGAS at Y214/215 affected cGAS activity. To confirm this, we reconstituted wild-type murine cGas ($mcGas^{WT}$) or its mutant $mcGas^{Y200/201F}$ (Y200/Y201 of mcGas correspond to Y214/Y215 of human cGAS) into cGas-deficient Raw264.7 cells. qPCR experiments indicated that transcription of the *Ifnb1* gene induced by HSV-1 infection, HT-DNA transfection, and A/Q treatment was restored in mcGas- but impaired in $mcGas^{Y200/201F}$-reconstituted cells (Fig. 3*B*). These results suggest that phosphorylation of $mcGas^{Y200/201}$ ($hcGAS^{Y214/215}$) is important for its activity. In vitro DNA-pulldown experiments showed that mutation of $hcGAS^{Y214/215F}$ bound to DNA, similar to wild-type hcGAS (Fig. 3*C*). However, mutation of Y214/215 of hcGAS to phenylalanine impaired formation of cGAS-DNA foci following HT-DNA transfection, which is a specific structure of liquid–liquid phase separation required for cGAS activation (7) (Fig. 3*D*). Consistently, SYK inhibitor PRT062607 treatment also markedly impaired HT-DNA transfection-induced formation of cGAS-DNA foci (Fig. 3*E*). Collectively, these results suggest that phosphorylation of $hcGAS^{Y214/215}$ ($mcGasY^{200/201}$) by SYK regulates phase separation of cGAS.

In past years, several studies suggest that the majority of cGAS localizes to the nucleus, with some cGAS in the cytoplasm in some cell types, such as L929 and HeLa (25–30). In our confocal microscopy experiments, cGas was indeed mainly localized in the nucleus in L929 cells (*SI Appendix*, Fig. S3*A*). However, in similar experiments, we observed that the majority of cGas was localized in the cytoplasm in Raw264.7 cells (*SI Appendix*, Fig. S3*A*), and the antibody used for cGas staining was validated with cGas-deficient cells (*SI Appendix*, Fig. S3*B*). It has also been reported that nuclear cGAS suppresses homologous recombination-mediated DNA repair (24). In this context, phosphorylation of cGAS at Y215 by BLK may maintain the cytosolic localization of cGAS, whereas stimulation with DNA-damaging agents leads to cGAS dephosphorylation and therefore facilitates the shuttling of cGAS to the nucleus (24). Therefore, we wondered whether phosphorylation of mouse cGas at Y201 (corresponding to Y215 of human cGAS) by Syk or Blk also regulates DNA damage-triggered nuclear translocation of cGas in Raw264.7 cells. However, the subcellular fractionation analysis indicated that irradiation had no marked effect on cytoplasmic (S0.8K) and nuclear (P0.8K) distribution of cGas in Raw264.7 cells, which indicated that irradiation-induced DNA damage might not trigger nuclear translocation of cGas in Raw264.7 cells. Furthermore, we also noticed that subcellular distribution of cGas was not affected by either Syk- or Blk-deficiency in these cells (*SI Appendix*, Fig. S3 *C* and *D*). Additionally, Syk- or Blk-deficiency hardly affected the recruitment of Rad51 (a critical homologous recombination factor) to DNA double-stranded breaks in response to DNA damage by irradiation (*SI Appendix*, Fig. S3*E*). These results suggest that Syk-mediated phosphorylation of cGas is not involved in homologous-recombination–mediated DNA repair in Raw264.7 cells.

The V-ATPase Mediates SYK Activation during Endocytosis of Foreign DNA. We next investigated how SYK is activated during endocytosis of foreign DNA. We sought for SYK-interacting proteins that are located at the plasma or endosomal membrane by biochemical purification and quantitative MS (*SI Appendix*, Fig. S4*A*). These efforts identified 16 candidate proteins located at the plasma membrane and 5 at the endosomal membrane (Fig. 4*A* and *SI Appendix*, Fig. S4*B*). Among these candidates, overexpression of several proteins—including ATP6V1A, FYN, and LYN—dramatically activated human SYK, which is indicated by phosphorylation of $hSYK^{Y525/526}$ (corresponding to Y519/520 of mouse Syk) (Fig. 4*B*). The tyrosine kinases FYN and LYN have been shown to directly mediate phosphorylation of SYK (31). ATP6AV1 is a protein in the peripheral V_1 domain of the V-ATPase, an endosomal or lysosomal membrane-associated proton pump (32) (Fig. 4*C*). It has been reported that the small chemical compound EN6 can be covalently conjugated to Cys277 of ATP6V1A, leading to disruption of the association of ATP6V1A with components of the other cytoplasmic complexes (33). In addition, Bafilomycin A1 (Baf-A1) is a macrolide antibiotic that binds to V0 domain of the V-ATPase and causes disassembly of the V-ATPase complex (34). Since V-ATPase is essential for cell survival (35), we used these inhibitors to examined the potential role of V-ATPase in SYK activation upon endocytosis of foreign DNA. We found that mouse Syk was recruited to the V-ATPase complex half an hour after HSV-1 infection (Fig. 4*D*). Overexpression of the majority of components in the peripheral V_1 domain of the V-ATPase could activate SYK (Fig. 4*E*). In addition, HSV-1 infection dramatically induced phosphorylation of mouse $Syk^{Y519/520}$ at 1 h postinfection and phosphorylation of mouse $cGas^{Y201}$ at 1 to 4 h postinfection, which were markedly impaired by blocking the V-ATPase complex with EN6 or Baf-A1 treatment (Fig. 4*F*). During our research, we routinely observed that HSV-1 infection-induced $p\text{-}mcGas^{Y201}$ started at 1 h but was greatly enhanced at 4 h postinfection (Fig. 4*F*). This probably indicates a second wave of phosphorylation of mouse cGas at Y201 at this time point, which might be caused by much enhanced association of Syk and cGas at 4 h (Fig. 2*G*) and a second wave of Syk activation at 4 h (Figs. 2*I* and 4*F*). Collectively, these results suggest an essential role of V-ATPase in activation of Syk and the subsequent phosphorylation of mouse $cGas^{Y201}$ following HSV-1 infection.

The V-ATPase Acts as a Scaffold for SYK-Mediated cGAS Priming at the Early Endosomes. It has been reported that cGAS is associated with the plasma membrane in phagocytes (15) and the V-ATPase complex assembles at early endosome during endocytosis (35). In light of our above results showing that mouse Syk was recruited to the V-ATPase complex at half an hour after HSV-1 infection (Fig. 4*D*) and recruited to mouse cGas at 2 to 4 h after HSV-1 infection (Fig. 2*G*), we hypothesized that the V-ATPase complex acts as a scaffold for SYK-cGAS association at early endosomes, which conditions it for proximal activation of cGAS by SYK. Confocal microscopy indicated that human cGAS was partially localized at the early endosomes but not lysosomes, the ER, and Golgi (*SI Appendix*, Fig. S5). Transient transfection and

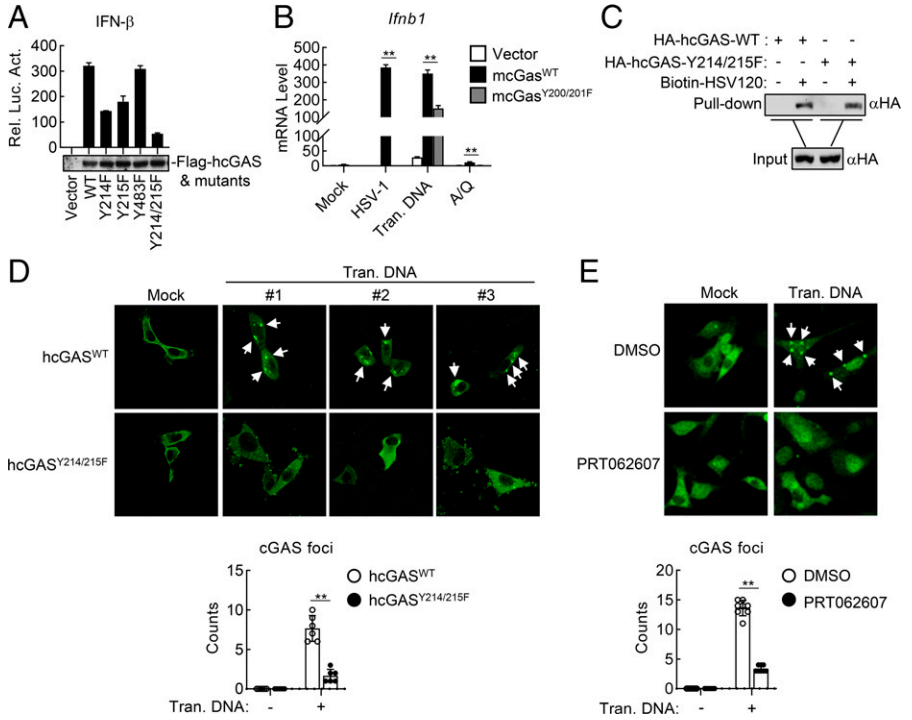

Fig. 3. Phosphorylation of cGAS at Y214/215 is critical for cGAS activation. (*A*) Effects of human cGAS and its mutants on IFN-β activation. The MITA/STING stably transduced HEK293 cells were transfected with the indicated plasmids together with an IFN-β reporter for 20 h before luciferase assays were performed. (*B*) Examination of endocytosed foreign DNA-induced transcription of the *Ifnb1* gene in reconstituted cGas-deficient cells. The indicated reconstituted cGas-deficient Raw264.7 cells (1×10^6) were treated with HSV-1 (MOI = 1) for 6 h, transfected with HT-DNA (1 μg/mL) for 4 h, or treated with A/Q (10 μM each) for 6 h before qPCR analysis of the *Ifnb1* gene. (*C*) Binding of human cGAS and its mutant to double-stranded DNA (dsDNA). HEK293 cells (1×10^7) were transfected with the indicated plasmids for 20 h, and then the cell lysates were incubated with biotinylated-HSV120 as well as streptavidin-Sepharose beads for in vitro pull-down assays. The bound proteins were then analyzed by immunoblots with the indicated antibody. (*D*) Effect of mutation of Y214/215 of human cGAS on the formation of cGAS foci. HT1080 cells were transfected with the indicated plasmids for 20 h before cells were left mock-transfected or transfected with dsDNA (HT-DNA, 1 μg/mL) for 3 h, and then fixed for immunofluorescent analysis. One representative field from mock-transfected cells and three representative fields from dsDNA-transfected cells are shown (*Upper*). The arrows indicate "cGAS foci". The average dots of "cGAS foci" in microscope fields ($n = 6$) were calculated and shown (*Lower*). (*E*) Effect of SYK inhibitor on the formation of cGAS foci. cGAS-GFP stably transduced HT1080 cells were pretreated with DMSO or PRT062607 (10 μM) for half an hour, and then left mock-transfected or transfected with dsDNA (HT-DNA, 1 μg/mL) for 3 h, and then fixed for microscopy analysis. One representative field from mock-transfected and dsDNA-transfected cells are shown (*Upper*). The arrows indicate "cGAS foci". The average dots of "cGAS foci" in microscope fields ($n = 8$) were calculated and shown (*Lower*). $^{**}P < 0.01$ (unpaired *t* test). The data shown are the mean ± SD ($n = 3$). All experiments were performed at least two times.

coimmunoprecipitation experiments indicated that human cGAS was associated with various components in the V-ATPase complex, especially strongly with membrane-embedded components of the V0 domain including ATP6V0A1, ATP6V0A2, and ATP6V0C (Fig. 5*A*). Furthermore, the association between human cGAS and SYK was markedly enhanced by overexpression of ATP6V1C and ATP6V1H, two peripheral components of the V-ATPase complex that are critically involved in the assembly of the V1 and V0 domains of the V-ATPase complex (36) (Fig. 5*B*). Consistently, treatment of cells with the V-ATPase inhibitor EN6 impaired the association of human SYK and ATP6V1A, as well as association of human SYK with cGAS (Fig. 5*C*). These results suggest that the V-ATPase acts as a scaffold for SYK-mediated priming of cGAS activation at the early endosomes.

Consistently, the V-ATPase inhibitor EN6 or Baf-A1 markedly inhibited cGAMP production and transcription of the *Ifnb1* gene induced by HT-DNA transfection in Raw264.7 cells (Fig. 5 *D* and *E*). The V-ATPase inhibitors also inhibited HSV-1–induced transcription of the *Ifnb1* gene and phosphorylation of $Irf3^{S388}$ (Fig. 5 *E* and *F*), but had no marked effects on A/Q-induced transcription of the *Ifnb1* gene in similar experiments (Fig. 5*E*). Transient knockdown of Atp6v1a and Atp6v1d by the CRISPR-Cas9 method inhibited HSV-1–induced transcription of *Ifnb1* and *Cxcl10* genes (Fig. 5*G*), but had no marked effects on IFN-γ–induced transcription of the *Irf1* gene in Raw264.7 cells (Fig. 5*H*). Additionally, inhibition of V-ATPase also suppressed transcription of antiviral genes induced by HSV-1 and HT-DNA transfection in THP-1 cells (*SI Appendix*, Fig. S6). These results suggest that the V-ATPase is critical for endocytosed DNA-triggered innate immunity.

Dual-Signal Model for Effective Activation of cGAS. According to our investigation above, we demonstrate that endocytosis of foreign DNA initiates the V-ATPae-SYK axis to prime cGAS activation. We further wondered whether activation of the V-ATPase-SYK axis is dependent of DNA binding to cGAS. The widely used transfection reagents, such as LF 2000 (LF2000) and PEI, are endocytosed from the extracellular environment into endosomes and then disturb the endosomal membrane in a low pH-dependent manner to release the cargoes (4, 37). Our recent study suggests that in the absence of foreign DNA cargo, LF2000 itself is sufficient to trigger a mild activation of cGAS-MITA/STING–dependent innate immunity by induction of Ca^{2+}-dependent mitostress and subsequent endogenous mtDNA release into cytosol (16, 17). Our following experiments indicated that LF2000 treatment also activates the V-ATPase-SYK axis, which is critical for LF2000-induced innate immunity.

As shown in Fig. 6*A*, the V-ATPase and SYK inhibitors markedly inhibited LF2000-induced cGAMP production in Raw264.7 cells. Treatment of the V-ATPase inhibitors or transient knockdown of Atp6v1a or Atp6v1d in the V-ATPase complex caused a dramatic decrease of LF2000-induced transcription of the

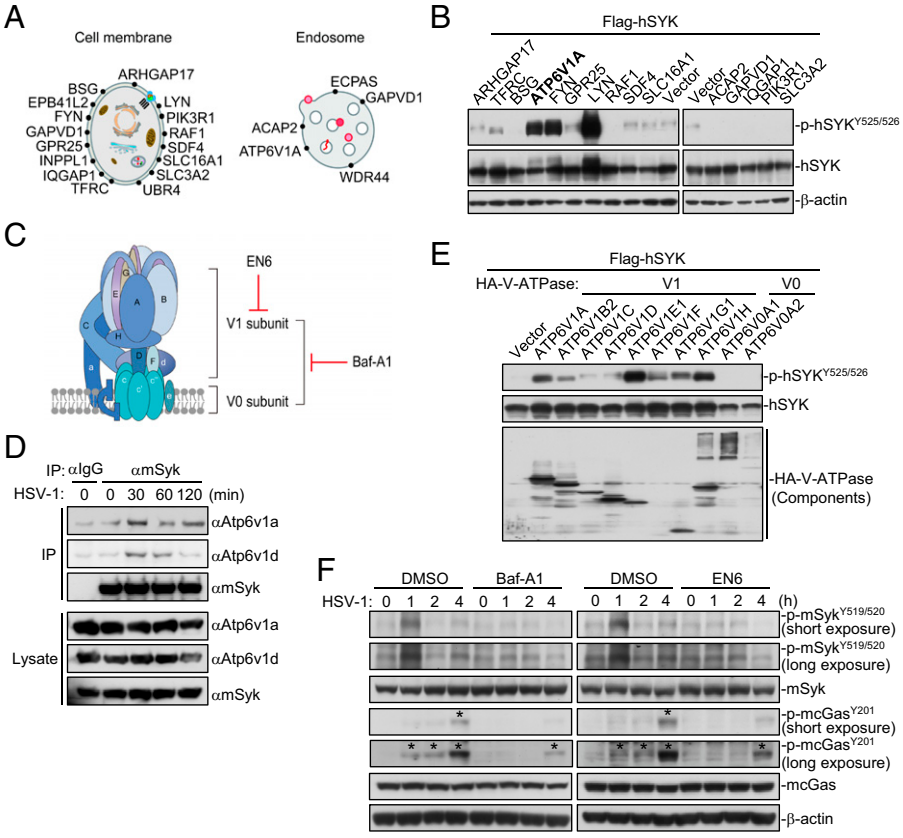

Fig. 4. The V-ATPase mediates SYK activation during endocytosis of foreign DNA. (*A*) Schematic diagrams for human SYK-associated membrane proteins identified by MS. (*B*) Biochemical screens for candidates that activate human SYK. HEK293 cells (1×10^6) were transfected with the indicated plasmids for 20 h and then lysed for immunoblot analysis with the indicated antibodies. (*C*) Schematic diagram of the composition in the V-ATPase complex. (*D*) Association of endogenous mouse Syk with V-ATPase. Raw264.7 cells (5×10^7) were left uninfected or infected with HSV-1 (MOI = 2) for the indicated times, and then lysed for coimmunoprecipitation with IgG or Syk antibody, followed by immunoblot analysis with the indicated antibodies. (*E*) Activation of the human SYK by V-ATPase. HEK293 cells (1×10^6) were transfected with the indicated plasmids for 20 h and then lysed for immunoblot analysis with the indicated antibodies. (*F*) Effects of V-ATPase inhibitors on HSV-1–induced activation of Syk and phosphorylation of cGas^{Y201}. RAW264.7 cells (1×10^6) were pretreated with DMSO, EN6 (30 μM), or Baf-A1 (20 nM) for half an hour, and then left uninfected or infected with HSV-1 (MOI = 2) for the indicated times before immunoblot analysis with the indicated antibodies. An asterisk (*) indicates detected signal of p-mcGas^{Y201}. All experiments were performed at least two times.

Ifnb1 gene (Fig. 6*B* and *SI Appendix*, Fig. S7*A*). Syk-deficiency also caused a marked decrease of LF2000-induced transcription of the *Ifnb1* gene in Raw264.7 cells (Fig. 6*C*). Similar results were observed in experiments performed with THP-1 cells (*SI Appendix*, Fig. S7 *B* and *C*). Furthermore, the V-ATPase inhibitors and SYK-deficiency impaired LF2000-induced phosphorylation of Tbk1^{S172} and Irf3^{S388} (*SI Appendix*, Fig. S7 *D* and *E*). These results suggest that the V-ATPase-SYK axis is critically involved in LF2000-induced innate immune response. LF2000 treatment induced phosphorylation of mouse Syk$^{Y519/520}$ and cGas^{Y201} in Raw264.7 cells, which was markedly down-regulated by treatment of the V-ATPase inhibitor EN6 (Fig. 6*D*). Similarly, Syk-deficiency also impaired LF2000-induced phosphorylation of mcGas^{Y201} (Fig. 6*E*). Collectively, all of these results suggest that the V-ATPase-SYK axis-mediated cGAS priming is also critically involved in LF2000-induced innate immune response. Finally, we examined whether mtDNA release is required for SYK-V-ATPase–mediated priming of cGAS following LF2000 treatment. Depletion of intracellular mtDNA by ddC, which is an inhibitor of mitochondrial DNA polymerase-γ and does not affect the function of nuclear DNA polymerases (38), caused an expected decrease of intracellular mtDNA copies (Fig. 6*F*) and transcription of the *Ifnb1* gene induced by LF2000 treatment (Fig. 6*G*). However, mtDNA depletion by ddC had no marked effects on LF2000-indued phosphorylation of mouse Syk$^{Y519/520}$ and cGas^{Y201} (Fig. 6*H*). These results suggest that the V-ATPase-SYK axis-mediated priming of cGAS activation is independent of its binding to DNA, which implies that cGAS priming and DNA binding are two essential but independent signals. We then examine whether combination of these two signals could achieve effective and potent cGAS-mediated innate immunity. As shown in Fig. 6*I*, either endogenous mtDNA release induced by A/Q or treatment of transfection reagents including LF2000 and PEI triggered a mild induction of *Ifnb1* and *Cxcl10* in Raw264.7 cells, but combination of A/Q with either LF2000 or PEI caused much more potent transcription of these antiviral genes, which suggests that a combination of the priming signal and DNA stimulation signal leads to robust innate immune response.

Based on our results, we propose a dual-signal model for effective activation of cGAS-mediated innate immune response (Fig. 6*J*). Following DNA virus infection or other triggers of endocytosis, the cargos are endocytosed to the early endosomes where the V-ATPase is assembled for acidation of the early endosomes. Then SYK and cGAS are recruited to the V-ATPase, where SYK is firstly activated and then phosphorylate human cGAS at Y214/215 (corresponding to Y200/201 of mouse cGas), which serves as a priming signal for cGAS activation. The binding of Y214/215-phosphorylated human cGAS to DNA (invaded viral DNA, transfected foreign DNA, released mtDNA, or dislocated cellular DNA) causes their efficient phase separation, leading to potent production of cGAMP and subsequent MITA/STING-dependent innate immune response.

Discussion

The cGAS-MITA/STING–mediated innate immunity plays an essential role in host defense against DNA viral infection (5). How cell membrane-associated molecular events govern cGAS-MITA/STING–mediated innate immunity upon viral invasion remains elusive. By screening a pool of tyrosine kinase inhibitors, we identified SYK as an important regulator for cGAS-mediated innate immunity triggered by endocytosed foreign DNA. We also found that SYK mediated tyrosine phosphorylation of human cGAS$^{Y214/215}$ (mouse cGas$^{Y200/201}$), which is important for formation of cGAS-DNA foci, a specific structure

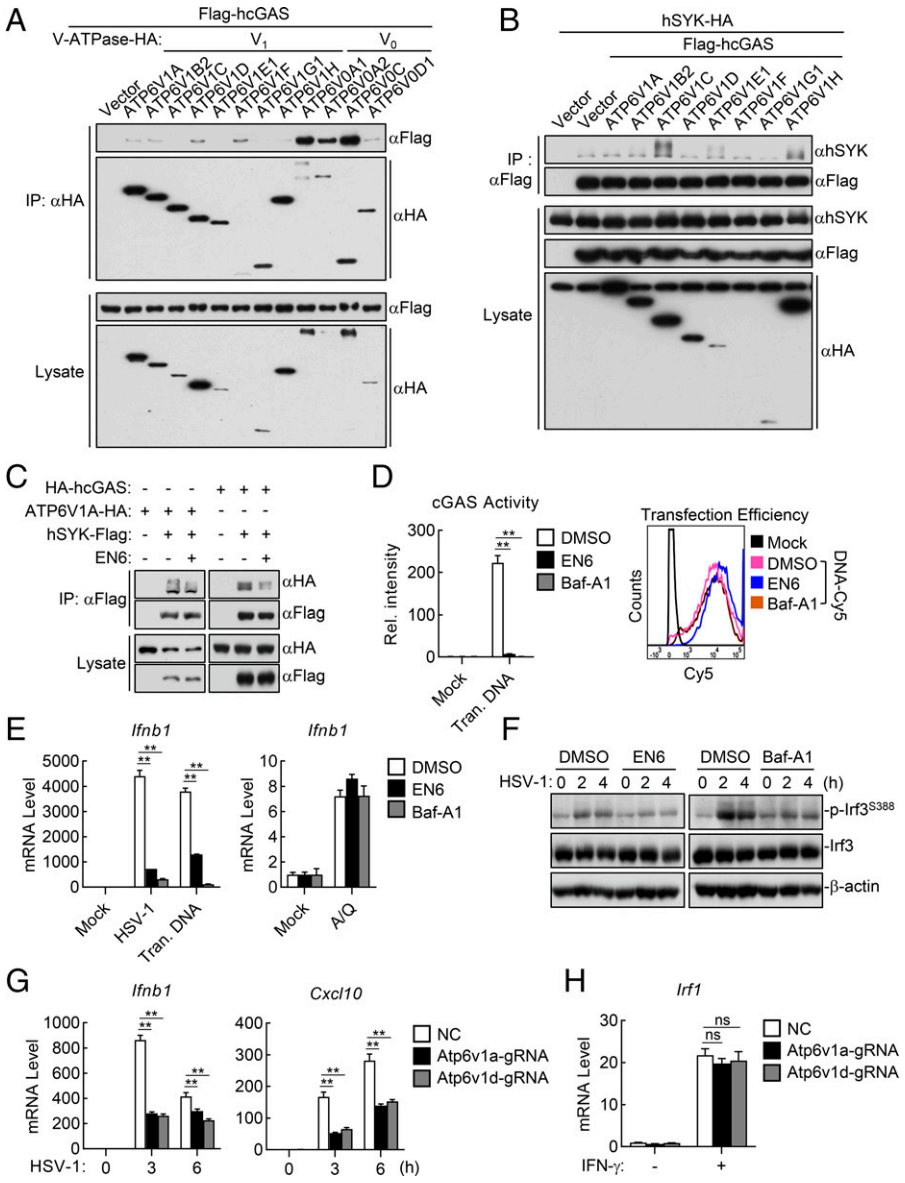

Fig. 5. The V-ATPase acts as a scaffold for SYK-mediated cGAS priming at the early endosomes. (*A*) Interaction of cGAS with components of the V-ATPase. HEK293 cells (1×10^7) were transfected with the indicated plasmids for 20 h and then lysed for coimmunoprecipitation with HA antibody, followed by immunoblot analysis with the indicated antibodies. (*B*) Effects of overexpression of individual component of V-ATPase on association between human SYK and cGAS. HEK293 cells (1×10^7) were transfected with the indicated plasmids for 20 h, and then lysed for coimmunoprecipitation with Flag antibody, followed by immunoblot analysis with the indicated antibodies. (*C*) Effects of V-ATPase inhibitor on human SYK-ATP6VA1 and SYK-cGAS association. HEK293 cells (1×10^7) were transfected with the indicated plasmids for 12 h before cells were left untreated or treated with EN6 (30 μM) for 10 h, and then cells were lysed for coimmunoprecipitation with Flag antibody, followed by immunoblot analysis with the indicated antibodies. (*D*) Effects of V-ATPase inhibitors on cGAS activity. Raw264.7 cells were pretreated with DMSO, EN6 (30 μM), or Baf-A1 (20 nM) for half an hour, and then mock-transfected or transfected with DNA-Cy5 (1 μg/mL) for 4 h, followed by cGAMP activity assay. The DNA transfection efficiency in each group is displayed (*Right*). (*E*) Effects of V-ATPase inhibitors on endocytosed foreign DNA-induced transcription of the *Ifnb1* gene. Raw264.7 cells (1×10^6) were pretreated with DMSO, EN6 (30 μM), or Baf-A1 (20 nM) for half an hour, and then treated with HSV-1 (MOI = 1) for 6 h, transfected with HT-DNA (1 μg/mL) for 4 h, or treated with A/Q (10 μM each) for 6 h, followed by qPCR analysis of the *Ifnb1* gene. (*F*) Effects of V-ATPase inhibitors on viral infection-induced phosphorylation of Tbk1 and Irf3. Raw264.7 cells (1×10^6) were pretreated with DMSO, EN6 (30 μM), or Baf-A1 (20 nM) for half an hour, and then left uninfected or infected with HSV-1 (MOI = 2) for the indicated times, followed by immunoblot analysis with the indicated antibodies. (*G* and *H*) Effects of transient knockdown of Atp6v1a and Atp6v1d on HSV-1– or IFN-γ–induced transcription of downstream genes. Raw264.7 cells (1×10^6) were transiently transfected with the indicated CRISPR-Cas9 vectors for 60 h, and then infected with HSV-1 (MOI = 1) for the indicated times (*G*) or treated with IFN-γ (100 ng/mL) for 4 h (*H*), followed by qPCR analysis of the indicated genes. ns, nonsignificant; $^{**}P < 0.01$ (unpaired *t* test). The data shown are the mean ± SD ($n = 3$). All experiments were performed at least two times.

of liquid–liquid phase separation required for cGAS activation (7). Through a biochemical purification approach, we next identified the endosomal H^+ pump V-ATPase as an activator of SYK, and we further found that V-ATPase also acts as a scaffold for SYK-mediated cGAS priming. Finally, by utilizing a specific immunostimulatory reagent LF2000, we demonstrate that the V-ATPase-SYK axis acts as a priming signal for cGAS upstream of DNA ligand binding. Therefore, we put forward a dual-signal model, in which both the first priming signal and the second DNA ligand binding signal are important for effective cGAS activation. These findings reveal key molecular events upstream of cGAS activation and provide evidence for a direct link between the endocytosis-triggered V-ATPase-SYK axis and innate immunity.

Multiple biological functions of V-ATPase have been elucidated in past decades. For example, by altering the pH of intracellular compartments and transmembrane electrical potential, the V-ATPase regulates enzymatic activity, ligand–receptor interaction, and coupled transport of substrates across membranes (3). The V-ATPase also acts as a signal component for signal transduction in regulation of a variety of other cellular processes, including fusogenicity, cytoskeletal tethering, metabolic sensing, developmental signaling, and bacterial xenophagy, which is independent of its ability as a proton pump (34, 39, 40). Our investigation reveals a function of V-ATPase in cGAS-mediated innate immunity. Actually, by maintaining the low pH of lysosome, V-ATPase plays an important role in cleanup of invaded virus that fails to escape from endosome, which is an intrinsic host defense strategy against viral infection (1, 34, 35). Furthermore, V-ATPase has been reported to act an autophagic receptor for xenophagy, which is also important for host defense against infection (40). Therefore, V-ATPase seems to act as a "commander-in-chief" that governs several different "armies" of host defense in cells. Whether and how V-ATPase is temporally and spatially regulated to coordinate all these different "armies" to achieve an optimal outcome of host defense remains elusive.

The tyrosine kinase SYK has been reported to regulate different biological processes, including innate and adaptive immunity, cell adhesion, osteoclast maturation, platelet activation, and

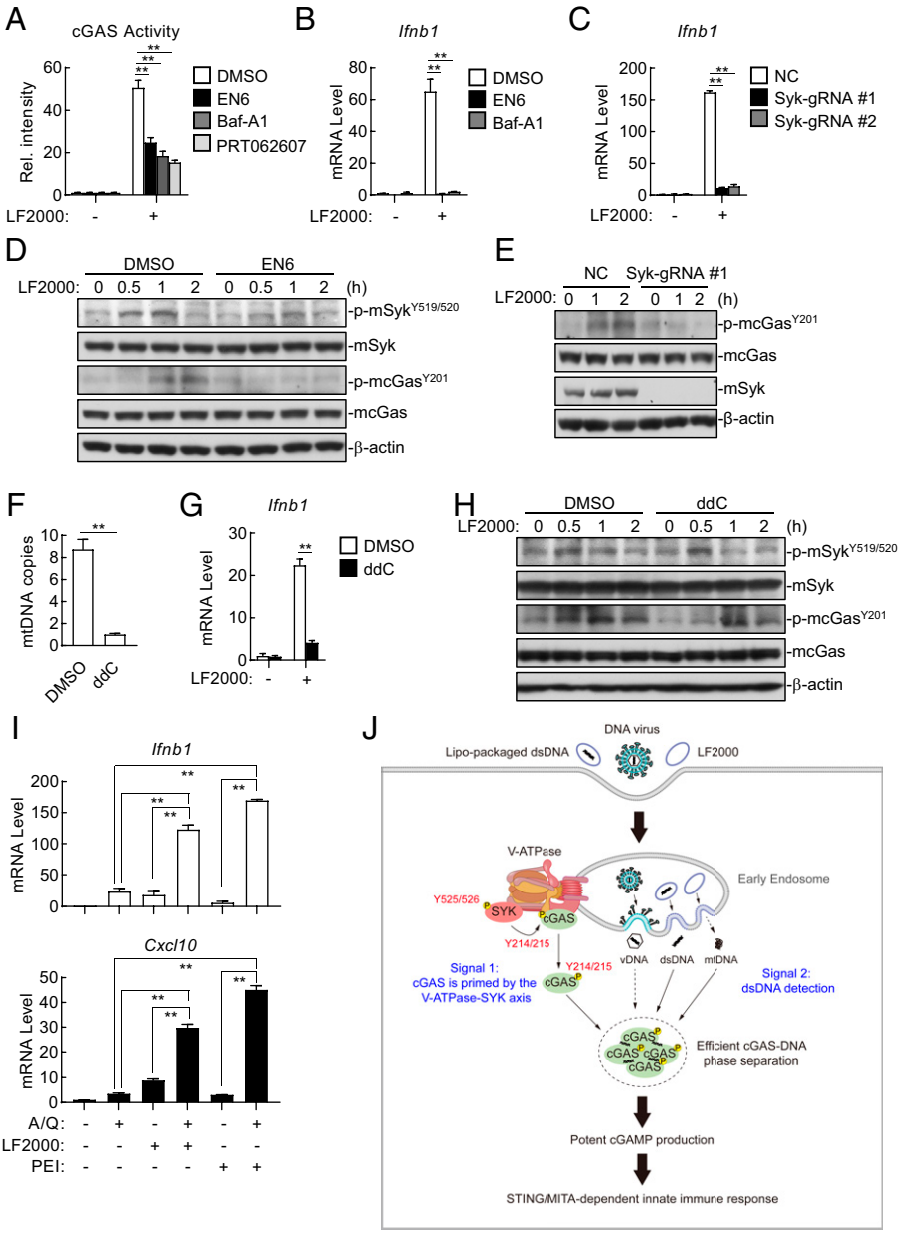

Fig. 6. LF2000 triggers V-ATPase-SYK axis for cGAS priming. (*A*) Effects of V-ATPase and SYK inhibitors on LF2000-induced cGAMP production. Raw264.7 cells (2×10^7) were pretreated with DMSO, EN6 (30 μM), Baf-A1 (20 nM), or PRT062607 (10 μM) for half an hour, and then untreated or treated with LF2000 (10 μg/mL) for 4 h, followed by cGAMP activity assay. (*B*) Effects of V-ATPase inhibitors on LF2000-induced transcription of the *Ifnb1* gene. Raw264.7 cells (1×10^6) were pretreated with DMSO, EN6 (30 μM), or Baf-A1 (20 nM) for half an hour, and then untreated or treated with LF2000 (10 μg/mL) for 6 h, followed by qPCR analysis of the *Ifnb1* gene. (*C*) Effects of Syk-deficiency on LF2000-induced transcription of the *Ifnb1* gene. The NC and Syk-deficient Raw264.7 cells (1×10^6) were untreated or treated with LF2000 (10 μg/mL) for 6 h, followed by qPCR analysis of the *Ifnb1* gene. (*D*) Effects of V-ATPase inhibitor on LF2000-induced activation of Syk and phosphorylation of cGas^{Y201}. RAW264.7 cells (1×10^6) were pretreated with DMSO or EN6 (30 μM) for half an hour, and then left untreated or treated with LF2000 (20 μg/mL) for the indicated times before immunoblot analysis with the indicated antibodies. (*E*) Effect of Syk-deficiency on LF2000-induced phosphorylation of cGas^{Y201}. The NC and Syk-deficient Raw264.7 cells (1×10^6) were treated with LF2000 (20 μg/mL) for the indicated times before immunoblot analysis with the indicated antibodies. (*F*) Measurement of the mtDNA depletion efficiency. Raw264.7 cells were treated with DMSO or ddC (50 ng/mL) for 5 d prior to DNA extraction and qPCR analysis. Data shown are the relative abundance of mitochondrial DNA (*D-loop*) normalized to that of genomic DNA (*Tert*). (*G*) Effect of mtDNA depletion on LF2000-induced transcription of the *Ifnb1* gene. DMSO and ddC (50 ng/mL)-treated Raw264.7 cells (1×10^6) were untreated or treated with LF2000 (10 μg/mL) for 6 h, followed by qPCR analysis of the *Ifnb1* gene. (*H*) Effects of mtDNA depletion on LF2000-induced activation of Syk and phosphorylation of cGas^{Y201}. DMSO and ddC (50 ng/mL)-treated Raw264.7 cells (1×10^6) were left untreated or treated with LF2000 (20 μg/mL) for the indicated times before immunoblot analysis with the indicated antibodies. (*I*) Combination of A/Q with LF2000- or PEI-induced transcription of *Ifnb1* and *Cxcl10* genes. Raw264.7 cells (1×10^6) were left untreated or treated with A/Q (10 μM each), LF2000 (10 μg/mL), or PEI (10 μg/mL) for 6 h, followed by qPCR analysis of the indicated genes. (*J*) Schematic diagram for "dual-signal" activation of cGAS-mediated innate immunity. $^{**}P < 0.01$ (unpaired *t* test). The data shown are the mean ± SD ($n = 3$). All experiments were performed at least two times.

vascular development (41). In these biological processes, SYK directly phosphorylates multiple downstream effectors, including VAV1, PLCG1, PI-3-kinase, LCP2, and BTK (41). In this study, we have identified cGAS as a phosphorylation substrate of SYK and established a direct link between SYK activation and cGAS priming. We suggest that SYK targets human cGAS$^{Y214/215}$ (mouse cGas$^{Y200/201}$) for tyrosine phosphorylation, which critically regulates the formation of cGAS-DNA foci, a specific structure of liquid–liquid phase separation required for cGAS activation (7). The DNA-pull down assay indicated that mutation of Y214/215 had no marked effect on DNA binding activity of human cGAS in vitro. How this phosphorylation event affects cGAS-DNA phase separation needs further exploration. Perhaps phosphorylation of these two residues aids to recruitment of certain accessory proteins involved in cGAS phase separation. In our study, we found that Syk-deficiency hardly affected cGAMP-induced transcription of antiviral genes, including *Ifnb1*, *Ifit1*, and *Cxcl10*, as well as activation of MITA/STING-mediated signaling that was indicated by phosphorylation of Mita^{S365}, Tbk1^{S172}, and Irf3^{S388} in Raw264.7 cells. These data clearly suggest that it is unlikely for Syk to function downstream of cGAMP in mouse macrophage Raw264.7 cells. A previous study reported that SYK mediates phosphorylation of MITA/STING at Y240 (42), which was conducted with L929, HT1080, and HeLa cells. Therefore, Syk might also regulate MITA/STING in epithelial cells or fibroblasts but not macrophages.

Through our exploration, we demonstrate that the endocytosis-triggered V-ATPase-SYK axis primes cGAS by mediating tyrosine phosphorylation of human cGAS$^{Y214/215}$ (mouse cGas$^{Y200/201}$). Either V-ATPase inhibitor treatment or Syk-deficiency decreased HSV-1 infection- and LF2000-induced p-cGas$^{Y200/201}$ levels in Raw264.7 cells. Consistently, reconstitution of wild-type mouse cGas but not its mutant cGas$^{Y214/215F}$ restored HSV-1 infection and transfected HT-DNA–induced transcription of *Ifnb1* in cGas-knockout (KO) cells. Interestingly, although the V-ATPase-SYK axis is not involved in endogenous mtDNA (A/Q)-induced innate immune response, we noticed that A/Q-induced transcription of *Ifnb1* in mcGas$^{Y200/201F}$-reconstituted cGas-KO

cells was much less than that of mcGas^{WT}-reconstituted cells, which suggests that phosphorylation of cGas$^{Y200/201}$ is also essential for endogenous mtDNA-induced innate immune response. Perhaps other kinases, such as Blk (24) but not Syk, mediate tyrosine phosphorylation of a fraction of mouse cGas at Y200/201 in resting cells. In this study, we identified Y214/215 as the major phosphorylated residues of cGAS by SYK in an overexpression system, and then we confirmed phosphorylation of endogenous murine cGas^{Y201} (corresponding to human cGAS^{Y215}) by SYK with a specific phosphorylation antibody. With this antibody, we detected that p-cGas^{Y201} was induced in control but not Syk-deficient cells after HSV-1 infection as well as LF2000 stimulation. However, confirmation of SYK-mediated phosphorylation of endogenous cGAS at Y214/215 by MS would further support our conclusion, which is not addressed in the present study.

During our exploration, we routinely found that p-mcGas^{Y201} was greatly enhanced at 4 h after HSV-1 infection. There are three possible reasons for this phenomenon. First, although the association of endogenous mcGas and Syk started at 1 h postinfection, their association was greatly enhanced at 4 h after HSV-1 infection in Raw264.7 cells. Second, it has been reported that type I IFN can stimulate the activity of Syk (43). Therefore, it is possible that type I IFN induced by HSV-1 infection at 4 h triggered a second wave of Syk activation, leading to the subsequent second wave of p-mcGas^{Y201} at 4 h after HSV-1 infection, which may serve as a positive feedback regulatory mechanism for mcGas activation. This is consistent with our observation of the kinetics of p-Syk$^{Y519/520}$ level following HSV-1 infection, which was peaked at 1 h and then decreased at 2 h, but increased at 4 h after HSV-1 infection. Third, type I IFN induced by HSV-1 infection at 4 h may also stimulate the activity of other tyrosine kinases to trigger a second wave of p-mcGas^{Y201} in Raw264.7 cells.

In this study, we suggest a dual-signal model for cGAS activation, in which both endocytosis-triggered V-ATPase-SYK axis-mediated cGAS priming and DNA ligand binding are required for effective cGAS activation. Importantly, this dual-signal model of cGAS activation makes it flexible for host cells to initiate differential immune response to DNA exposure in different situations. For example, upon DNA viral infection or endocytosis of foreign DNA, cGAS is fully primed during endocytosis, and then binds to cytosolic viral DNA or self-DNA (even if DNA level is low), which cause efficient cGAS-DNA phase separation, leading to potent production of cGAMP and MITA/STING-dependent innate immune response. However, in sterile situations where cGAS is not effectively primed by SYK-mediated tyrosine phosphorylation at Y214/215, host cells keep tolerant to cytosolic self-DNA (even if DNA level is high), and harmful autoimmunity can be avoided. Therefore, our findings also uncover a "proactive" protective strategy for host cells to avoid autoimmune response to self-DNA in sterile situations.

In addition to DNA viruses, the cGAS-MITA/STING signaling is also involved in innate immunity triggered by many RNA viruses (44). It is probably that endocytosis of RNA virus also activates the V-ATPase-SYK axis for cGAS priming, which leads to cGAS-mediated innate immune response once the primed cGAS senses cytosolic self-DNA. We also wondered whether the V-ATPase-SYK axis directly primes RIG-1–like receptors (RLR)- or Toll-like receptor-mediated innate immunity upon RNA viral infection. A recent study suggests that SYK plays an important role in RLR-mediated innate immune response to RNA viral infection by mediated tyrosine phosphorylation of STAT1 downstream of RIG-I-VISA/MAVS (45). Whether SYK mediates RLR or VISA/MAVS priming will be explored in the future.

In summary, our findings uncover the key molecular mechanism of endosomal V-ATPase-SYK–dependent cGAS priming during endocytosis, and suggest a dual-signal model for cGAS activation, which may provide new insights for drug design of infectious and autoimmune diseases.

Materials and Methods

Reagents, Viruses, and Cells. Purchased from the indicated manufacturers were: fetal bovine serum (SA211.02, Cellmax), penicillin and streptomycin (SV30010, HyClone), Dulbecco's modified Eagle's medium (C11965500BT, Gibco), puromycin (AMR-J593,VWR), neomycin (G418) (108321-42-2, Sigma-Aldrich), digitonin (11024-24-1, Sigma-Aldrich), 2′3′-cGAMP (tlrl-nacga23-02, Invitrogen), lipofectamine 2000 (11668019, Invitrogen), the reagents HT-DNA (D6898, Sigma), polybrene (TR-1003-G, Millipore), benzonase nuclease (20156ES50, YEASEN), dual-specific luciferase assay kit (E1980, Promega), SYBR Green supermix (1725124, Bio-Rad), HiScript II Select RT SuperMix for qPCR (R222-01, Vazyme), VeriKineTM mouse IFN-β ELISA (42400-2, PBL), and mouse IP-10/CXCL10 ELISA kit (EMC121, Neobioscience).

The inhibitors ABT-737 (HY-50907), Q-VD-OPh (HY-12305), PRT062607 (HY-15322), BAY 61-3606 dihydrochloride (HY-14985), Vecabrutinib (HY-109078), BMS-509744 (HY-11092), PRN1371 (HY-101768), BLZ945 (HY-12768), AG 1295 (HY-101957), RU.521 (HY-114180), STING-IN-3 (HY-138683), Baf-A1 (HY-100558), EN6 (HY-128892), and zalcitabine (HY-17392) were purchased from MCE; AZD4547 (T1948), FIIN-2 (T6836), and Orantinib (T6184), CP673451 (T6091) were purchased from Target Mol.

Mouse monoclonal antibodies against HA (TA180128, OriGene); rabbit monoclonal antibodies against HA (TA591010, OriGene); Flag (F3165, Sigma); ATP6V1A (ab199326, Abcam); ATP6V1D (ab157458, Abcam); ATP6V1H (SC-166227, Santa Cruz); p-cGAS^{Y215} (AP0946, ABclonal); mcGAS (31659, CST); hcGAS (15102, CST); SYK (13198, CST); p-SYK$^{Y525/526}$ (2710, CST); TBK1 (ab40676, Abcam); p-TBK1^{S172} (ab109272, Abcam); IRF3 (sc-33641, Santa Cruz); p-IRF3^{S396} (4947, CST); β-actin (A2228, Sigma); RAD51 (ab133534, Abcam); Lamin B (12987-1-AP, proteintech); β-tubulin (32-2600, Invitrogen); peroxidase AffiniPure Goat Anti-Rabbit IgG (H+L) (111-035-003, Jackson ImmunoResearch); goat anti-mouse IgG (H+L) Highly Cross-Adsorbed Secondary Antibody, Alexa Fluor Plus 488 (A32723, ThermoFisher Scientific); and Goat anti-Rabbit IgG (H+L) Highly Cross-Adsorbed Secondary Antibody, Alexa Fluor Plus 594 (A32740, ThermoFisher Scientific) were purchased from the indicated manufacturers.

HEK293, THP-1, and Raw264.7 cells were obtained from ATCC. HT1080 and BV2 were purchased from CCTC and CCTCC, respectively. BMDCs were prepared as described previously (46). HSV-1 were previously described (46).

Mice. C57/B6 mice were purchased from Model Animal Research Centre of Nanjing University and maintained in specific pathogen-free rooms. The viral infection experiments were performed in ABSL-2 laboratories. Experiments were conducted without blinding. All animal experiments were performed in accordance with the Wuhan University Medical Research Institute Animal Care and Use Committee Guidelines.

Constructs. Expression plasmids for HA- or FLAG-tagged SYK, hcGAS, mcGAS and their mutants, HA-tagged V-ATPase, and Flag-tagged Blk were constructed by standard molecular biology techniques.

Gene KO by CRISPR-Cas9. Double-stranded oligonucleotides corresponding to the target sequences were cloned into the lenti-CRISPR-V2 vector, which was cotransfected with packaging plasmids into HEK293 cells. Forty-eight hours after transfection, the viruses were harvested for infection of target cells. The infected cells were selected with puromycin for 6 d to establish stable cell lines, or for 2 d for transient knockdown of Atp6v1a or Atp6v1d, before cells were seeded for additional experiments. The following sequences were targeted for the indicated genes:

Mouse Syk-gRNA #1: 5′-GCGCATGATCGGAATCTGCG-3′;
Mouse Syk-gRNA #2: 5′-GGCACCTACGCCATCTCCGG-3′;
Mouse Atp6v1a-gRNA: 5′-GGCAGCGCCCGCCATGTCAC-3′;
Mouse Atp6v1d-gRNA: 5′-CTGACCGGTTTAGCCAGAGG-3′;

Mouse Blk-gRNA: 5′-CTGTGAATGACAGGGACCTT-3′;
Mouse cGas-gRNA: 5′-CGCAAAGGGGGGCTCGATCG-3′;
Human SYK-gRNA #1: 5′-CAACTACCTGGGTGGCTTC-3′;
Human SYK-gRNA #2: 5′-ACGGGAGGAAGGCACACCA-3′.

qPCR. Total RNAs were isolated and the reverse-transcribed products were obtained for qPCR analysis to measure mRNA levels of the indicated genes. Data shown are the relative abundance of the indicated mRNA normalized to that of *GAPDH*. The sequences of the qPCR primers were as follows:

Human *GAPDH*: 5′-GACAAGCTTCCCGTTCTCAG-3′ and 5′-GAGTCAACGGATTTGG TCGT-3′;
Human *IFNB1*: 5′-TGACTATGGTCCAGGCACAG-3′ and 5′-TTGTTGAGAACCTCC TGGCT-3′;
Human *IFIT1*: 5′-TCATCAGGTCAAGGATAGTC-3′ and 5′-CCACACTGTATTTGGTGTCT AGG-3′;
Human *CXCL10*: 5′-GGTGAGAAGAGATGTCTGAATCC-3′ and 5′-GTCCATCCTTGGA AGCACTGCA-3′;
Mouse *Gapdh*: 5′-ACGGCCGCATCTTCTTGTGCA-3′ and 5′-ACGGCCAAATCCGTTCA CACC-3′;
Mouse *Ifnb1*: 5′-TCCTGCTGTGCTTCTCCACCACA-3′ and 5′-AAGTCCGCCCTGTAGGTG AGGTT-3′;
Mouse *Ifit1*: 5′-ACAGCAACCATGGGAGAGAATGCTG-3′ and 5′-ACGTAGGCCAGGAGG TTGTGCAT-3′;
Mouse *Cxcl10*: 5′-ATCATCCCTGCGAGCCTATCCT-3′ and 5′-GACCTTTTTTGGCTAAA CGCTTTC-3′;
HSV-1 *UL1*: 5′- CCCTCTCCAAGGTTCCGTTC-3′ and 5′-TGCCTTTCAAACCGACCAGT-3′;
HSV-1 *UL49*: 5′-CGCACAGACGAAGACCTCAA-3′ and 5′-ACCACGTCTGGATTCACCAA-3′.

Viral Plaque Assay. Seven-week-old mice were infected with HSV-1 (KOS strain) for 4 to 6 d. The brains or brainstems of infected mice were harvested, weighed, and homogenized. Vero cells were seeded in 24-well plates, and the cells were infected by incubation for 2 h at 37 °C with serial dilutions of the suspensions. The infected cells were overlaid with 1.5% methylcellulose and were then incubated for 48 h. The cells were fixed with 4% paraformaldehyde and stained with 1% Crystal violet before plaque counting.

Transfection and Reporter Assays. HEK293 cells were transfected with the indicated plasmids by the calcium phosphate precipitation method. Luciferase assays were performed using a Dual-Specific Luciferase Assay Kit. To normalize for transfection efficiency, pRL-TK (*Renilla* luciferase) reporter plasmid (0.01 μg) was added to each transfection. Firefly luciferase activities were normalized with *Renilla* luciferase activities.

mtDNA Depletion. The Raw264.7 cells (1×10^6) were treated with DMSO or ddC (50 ng/mL) for 5 d to deplete mtDNA. To evaluate mtDNA depletion efficiency, DNA from the DMSO- or ddC-treated cells was extracted for qPCR analysis with primers corresponding to the mitochondrial gene *D-loop* and the nuclear genomic gene *Tert*. qPCR primers were previously reported (19).

Confocal Microscopy. The cells were seeded on coverslips in 24-well plates. After treatment, the cells were fixed with 4% paraformaldehyde for 20 min and then permeablized for 15 min by incubation with 0.1% Triton X-100. The cells were blocked in 1% BSA and stained with the indicated antibodies. Imaging of the cells was carried out using Zeiss LSM880 confocal microscope.

Coimmunoprecipitation and Immunoblot Analysis. Cells were lysed with lysis buffer (20 mM Tris·HCl, pH 7.5; 1% Nonidet P-40; 10 mM NaCl; 3 mM EDTA, and 3 mM EGTA, complete protease inhibitor mixture) at 4 °C for 10 min. The lysates were centrifugated at 13,000 rpm for 10 min at 4 °C. The supernatants were immunoprecipitated with the indicated antibodies and protein G magnetic beads and then incubated at 4 °C for 3 h. Then the beads were washed three times with washing buffer (500 mM NaCl, 50 mM Tris·HCl [pH 7.5]). The bound proteins were separated by SDS/PAGE, followed by immunoblotting analysis with the indicated antibodies.

In Vitro Pull-Down Assays. HEK293 cells transfected with the indicated plasmids were lysed in Triton X-100 lysis buffer. The lysates were incubated with biotinylated-HSV120 for 2 h at 4 °C and then incubated with streptavidin beads for 1 h at 4 °C. The beads were washed five times with lysis buffer (500 mM NaCl, 50 mM Tris·HCl [pH 7.5]) and analyzed by immunoblotting with the indicated antibodies.

cGAMP Activity Assay. Raw264.7 cells (2×10^7) were left untreated or transfected with HT-DNA or DNA-Cy5 for 4 h, and then cell extracts were prepared and heated at 95 °C for 10 min to denature most proteins, which were removed by centrifugation at 20,000 × *g* for 25 min at 4 °C. The supernatants containing cGAMP were delivered to Raw264.7 pretreated with digitonin permeabilization solution (50 mM Hepes pH 7.0, 100 mM KCl, 3 mM $MgCl_2$, 0.1 mM DTT, 85 mM Sucrose, 0.2% BSA, 1 mM ATP, 0.1 mM GTP and 10 μg/mL digitonin) at 37 °C for 30 min (46). Four hours later, the cells were collected for qPCR analysis. The transcription of *Cxcl10* was measured to represent cGAS activity.

Statistics Analysis. Unpaired Student's *t* test was used for statistical analysis with GraphPad Prism Software. For the mouse survival study, Kaplan–Meier survival curves were generated and analyzed by log-rank test. The number of asterisks represents the degree of significance with respect to *P* values. Statistical significance was set at $*P < 0.05$ or $**P < 0.01$.

Data, Materials, and Software Availability. All data are provided in the main text and *SI Appendix*.

ACKNOWLEDGMENTS. We thank Prof. Bo Zhong (Wuhan University), Prof. Hao Yin (Wuhan University), Prof. Qiang Chen (Wuhan University), Prof. Xuefeng Chen (Wuhan University), and Dr. Mi Li (Wuhan University) for constructive suggestions; and Simin Chen (Renmin Hospital of Wuhan University) for technical help of ocular infection of HSV-1 in mice. This work was supported by grants from the State Key R&D Program of China (2021YFA1302400), the National Natural Science Foundation of China (31922021, 32188101, 32170713, and 31830042), the Chinese Academy of Medical Sciences Innovation Fund for Medical Sciences (2019-I2M-5-071), and the Fundamental Research Funds for the Central Universities.

Author affiliations: [a]Department of Infectious Diseases, Medical Research Institute, Frontier Science Center for Immunology and Metabolism, Zhongnan Hospital of Wuhan University, Taikang Center for Life and Medical Sciences, State Key Laboratory of Virology, Wuhan 430071, China; and [b]Research Unit of Innate Immune and Inflammatory Diseases (2019RU063), Chinese Academy of Medical Sciences, Beijing 100730, China

1. C. S. Kumar, D. Dey, S. Ghosh, M. Banerjee, Breach: Host membrane penetration and entry by nonenveloped viruses. *Trends Microbiol.* **26**, 525–537 (2018).
2. M. Kielian, F. A. Rey, Virus membrane-fusion proteins: More than one way to make a hairpin. *Nat. Rev. Microbiol.* **4**, 67–76 (2006).
3. P. M. Kane, The where, when, and how of organelle acidification by the yeast vacuolar H+-ATPase. *Microbiol. Mol. Biol. Rev.* **70**, 177–191 (2006).
4. I. M. S. Degors, C. Wang, Z. U. Rehman, I. S. Zuhorn, Carriers break barriers in drug delivery: Endocytosis and endosomal escape of gene delivery vectors. *Acc. Chem. Res.* **52**, 1750–1760 (2019).
5. M. M. Hu, H. B. Shu, Innate immune response to cytoplasmic DNA: Mechanisms and diseases. *Annu. Rev. Immunol.* **38**, 79–98 (2020)..
6. A. Ablasser, Z. J. Chen, cGAS in action: Expanding roles in immunity and inflammation. *Science* **363**, eaat8657 (2019).
7. M. Du, Z. J. Chen, DNA-induced liquid phase condensation of cGAS activates innate immune signaling. *Science* **361**, 704–709 (2018).
8. L. Sun, J. Wu, F. Du, X. Chen, Z. J. Chen, Cyclic GMP-AMP synthase is a cytosolic DNA sensor that activates the type I interferon pathway. *Science* **339**, 786–791 (2013).
9. J. Wu *et al.*, Cyclic GMP-AMP is an endogenous second messenger in innate immune signaling by cytosolic DNA. *Science* **339**, 826–830 (2013).
10. H. Ishikawa, Z. Ma, G. N. Barber, STING regulates intracellular DNA-mediated, type I interferon-dependent innate immunity. *Nature* **461**, 788–792 (2009).
11. B. Zhong *et al.*, The adaptor protein MITA links virus-sensing receptors to IRF3 transcription factor activation. *Immunity* **29**, 538–550 (2008).
12. M. M. Hu, H. B. Shu, Cytoplasmic mechanisms of recognition and defense of microbial nucleic acids. *Annu. Rev. Cell Dev. Biol.* **34**, 357–379 (2018).
13. O. Takeuchi, S. Akira, Pattern recognition receptors and inflammation. *Cell* **140**, 805–820 (2010).
14. K. McArthur *et al.*, BAK/BAX macropores facilitate mitochondrial herniation and mtDNA efflux during apoptosis. *Science* **359**, eaao6047 (2018).
15. K. C. Barnett *et al.*, Phosphoinositide interactions position cGAS at the plasma membrane to ensure efficient distinction between self- and viral DNA. *Cell* **176**, 1432–1446.e11 (2019).
16. C. K. Holm *et al.*, Virus-cell fusion as a trigger of innate immunity dependent on the adaptor STING. *Nat. Immunol.* **13**, 737–743 (2012).

17. W. R. He *et al.*, VRK2 is involved in the innate antiviral response by promoting mitostress-induced mtDNA release. *Cell. Mol. Immunol.* **18**, 1186–1196 (2021).
18. M. J. White *et al.*, Apoptotic caspases suppress mtDNA-induced STING-mediated type I IFN production. *Cell* **159**, 1549–1562 (2014).
19. A. Rongvaux *et al.*, Apoptotic caspases prevent the induction of type I interferons by mitochondrial DNA. *Cell* **159**, 1563–1577 (2014).
20. S. E. Spurgeon *et al.*, The selective SYK inhibitor P505-15 (PRT062607) inhibits B cell signaling and function in vitro and in vivo and augments the activity of fludarabine in chronic lymphocytic leukemia. *J. Pharmacol. Exp. Ther.* **344**, 378–387 (2013).
21. G. Coffey *et al.*, Specific inhibition of spleen tyrosine kinase suppresses leukocyte immune function and inflammation in animal models of rheumatoid arthritis. *J. Pharmacol. Exp. Ther.* **340**, 350–359 (2012).
22. B. Roizman, D. M. Knipe, R. J. Whitley, "Herpes simplex viruses" in *Fields Virology*, D. M. Knipe, P. M. Howley, Eds. (Lippincott Williams & Wilkins, 2007), vol. 1, pp. 2501–2602.
23. L. S. Reinert *et al.*, Sensing of HSV-1 by the cGAS-STING pathway in microglia orchestrates antiviral defence in the CNS. *Nat. Commun.* **7**, 13348 (2016).
24. H. Liu *et al.*, Nuclear cGAS suppresses DNA repair and promotes tumorigenesis. *Nature* **563**, 131–136 (2018).
25. K. C. Barnett *et al.*, Phosphoinositide interactions position cGAS at the plasma membrane to ensure efficient distinction between self- and viral DNA. *Cell* **176**, 1432–1446.e11 (2019).
26. H. E. Volkman, S. Cambier, E. E. Gray, D. B. Stetson, Tight nuclear tethering of cGAS is essential for preventing autoreactivity. *eLife* **8**, e47491 (2019).
27. S. Michalski *et al.*, Structural basis for sequestration and autoinhibition of cGAS by chromatin. *Nature* **587**, 678–682 (2020).
28. B. Y. Zhao *et al.*, The molecular basis of tight nuclear tethering and inactivation of cGAS. *Nature* **587**, 673–677 (2020).
29. J. A. Boyer *et al.*, Structural basis of nucleosome-dependent cGAS inhibition. *Science* **370**, 450–454 (2020).
30. B. Guey *et al.*, BAF restricts cGAS on nuclear DNA to prevent innate immune activation. *Science* **369**, 823–828 (2020).
31. J. Rivera, A. M. Gilfillan, Molecular regulation of mast cell activation. *J. Allergy Clin. Immunol.* **117**, 1214–1225, quiz 1226 (2006).
32. C. A. Wagner *et al.*, Renal vacuolar H+-ATPase. *Physiol. Rev.* **84**, 1263–1314 (2004).
33. C. Y. Chung *et al.*, Covalent targeting of the vacuolar H^+-ATPase activates autophagy via mTORC1 inhibition. *Nat. Chem. Biol.* **15**, 776–785 (2019).
34. M. E. Maxson, S. Grinstein, The vacuolar-type H^+-ATPase at a glance–More than a proton pump. *J. Cell Sci.* **127**, 4987–4993 (2014).
35. M. Forgac, Vacuolar ATPases: Rotary proton pumps in physiology and pathophysiology. *Nat. Rev. Mol. Cell Biol.* **8**, 917–929 (2007).
36. T. Inoue, M. Forgac, Cysteine-mediated cross-linking indicates that subunit C of the V-ATPase is in close proximity to subunits E and G of the V1 domain and subunit a of the V0 domain. *J. Biol. Chem.* **280**, 27896–27903 (2005).
37. W. F. Lai, In vivo nucleic acid delivery with PEI and its derivatives: Current status and perspectives. *Expert Rev. Med. Devices* **8**, 173–185 (2011).
38. L. S. Kaguni, DNA polymerase gamma, the mitochondrial replicase. *Annu. Rev. Biochem.* **73**, 293–320 (2004).
39. G. H. Sun-Wada, Y. Wada, Role of vacuolar-type proton ATPase in signal transduction. *Biochim. Biophys. Acta* **1847**, 1166–1172 (2015).
40. Y. Xu *et al.*, A bacterial effector reveals the V-ATPase-ATG16L1 axis that initiates xenophagy. *Cell* **178**, 552–566.e20 (2019).
41. A. Mócsai, J. Ruland, V. L. Tybulewicz, The SYK tyrosine kinase: A crucial player in diverse biological functions. *Nat. Rev. Immunol.* **10**, 387–402 (2010).
42. C. Wang *et al.*, STING-mediated interferon induction by Herpes simplex virus 1 requires the protein tyrosine kinase Syk. *MBio* **12**, e0322821 (2021).
43. I. Tassiulas *et al.*, Amplification of IFN-alpha-induced STAT1 activation and inflammatory function by Syk and ITAM-containing adaptors. *Nat. Immunol.* **5**, 1181–1189 (2004).
44. L. G. Webb, A. Fernandez-Sesma, RNA viruses and the cGAS-STING pathway: Reframing our understanding of innate immune sensing. *Curr. Opin. Virol.* **53**, 101206 (2022).
45. S. Liu *et al.*, Critical role of Syk-dependent STAT1 activation in innate antiviral immunity. *Cell Rep.* **34**, 108627 (2021).
46. M. M. Hu *et al.*, Sumoylation promotes the stability of the DNA sensor cGAS and the adaptor STING to regulate the kinetics of response to DNA virus. *Immunity* **45**, 555–569 (2016).